Melt Pool Size and Stress Control for Laser-Based Deposition Near a Free Edge

Pruk Aggarangsi and Jack L. Beuth
Department of Mechanical Engineering
Carnegie Mellon University
Pittsburgh, PA

Michelle Griffith
Sandia National Laboratories
Albuquerque, NM

Abstract

Thermomechanical models developed in this research address two experimental observations made during the deposition of thin-walled structures by the LENS^{TM} process. The first observation (via thermal imaging) is of substantial increases in melt pool size as a vertical free edge is approached under conditions of constant laser power and velocity. The second observation (via neutron diffraction) is of large tensile stresses in the vertical direction at vertical free edges, after deposition is completed and the wall is allowed to cool to room temperature. At issue is how to best control melt pool size as a free edge is approached and whether such control will also reduce observed free edge stresses. Thermomechanical model results are presented which demonstrate that power reduction curves suggested by process maps for melt pool size under steady-state conditions can be effective in controlling melt pool size as a free edge is approached. However, to achieve optimal results it is important that power reductions be initiated before increases in melt pool size are observed. Stress simulations indicate that control of melt pool size can reduce free-edge stresses; however, the primary cause of these stresses is a constraint effect which is independent of melt pool size.

Introduction

The LENS^{TM} Process: The primary application of this work is to the Laser Engineered Net Shaping (LENS™) process developed at Sandia National Laboratories (Griffith et al., 1996). The LENS™ process is one of a number of competing processes developed with the goal of automatically fabricating complex shapes or features directly out of metal, based on a 3-D computer-aided-design model of the part. In the LENS™ process, parts are constructed by focusing a high-power laser beam onto a metal substrate, where it intersects streams of metallic powder. The laser locally melts the powder to form a molten pool on the top surface of the growing part. By moving the substrate under the laser beam, a part is built up, line by line and layer by layer. Parts are deposited onto a large metal base plate, which conducts heat away from the part, and acts to constrain the part from deformation during deposition. As shown in Fig. 1, the process is particularly well-suited for the construction of fine features such as thin-walled structures. The models developed in this research directly address the construction of thin-walled features. Work is underway to not only optimize LENS™ process parameters manually, but to use real-time thermal images of melt pool size as part of a feedback mechanism controlling the process (Griffith et al., 1999).
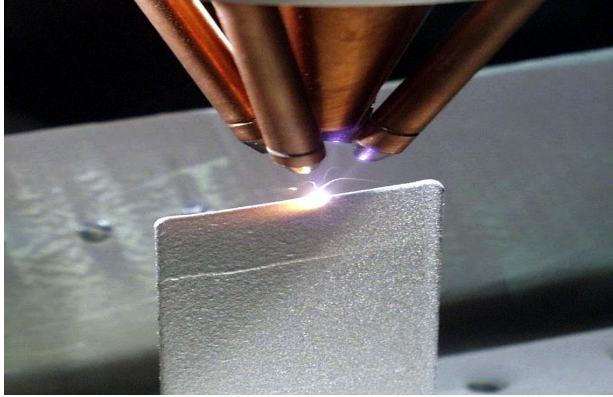
Figure 1 Image of the LENS™ process fabricating a thin-walled structure.

Problem Considered: The research described herein is motivated by two observations made during the construction of thin-walled features. The first observation comes from direct thermal imaging of the melt pool during metal deposition (Rangaswamy et al., 2003). Figure 2 shows experimentally obtained thermal contours as seen from the side of a stainless steel wall from such experiments. As the laser moves across the top of the wall with a constant laser power and velocity, the thermal contours reach a steady-state configuration (as viewed by an observer moving at the velocity of the laser). As a free surface is approached, however, the melt pool size becomes significantly larger, due to the decreased ability of the substrate to conduct heat away from the melt pool.

Precise control of melt pool size is essential for accurate deposition of thin-walled structures and a key issue is how laser power and/or velocity might be altered to maintain a constant melt pool size as a free edge is approached. The problem is exacerbated by the fact that a reduction in laser velocity (and thus an increase in thermal energy imparted to the wall per distance moved in the deposition direction) may be needed to accurately deposit material near free edges, where a velocity reversal is needed to continue with deposition of the next layer of material. Although critical for thin-walled structures, analogous problems exist as free edges are approached in the deposition of bulky structures.

A second observation serving as motivation for this research comes from neutron diffraction measurements of stress in thin-walled structures at a fixed depth from the deposition surface (Rangaswamy et al., 2003). Figure 3 shows a plot of measured stresses as a function of distance across the width of a deposited thin wall (where the width is measured in the deposition direction). Measurements are taken at a depth of 45 mm from the top surface of a wall that is 90 mm tall, 25.4 mm wide and 1.5 mm thick. The y coordinate is defined as being the horizontal coordinate along the direction of deposition (along the width), the x direction is defined as being the horizontal coordinate normal to the direction of deposition (through the thickness) and the z coordinate is in the vertical (height) direction. In contrast to stresses near the top of the wall, which consist of large stresses in the y (deposition) direction and essentially zero stress in the x and z directions, at a depth into the substrate there are large stresses in the z (vertical) direction and relatively small stresses in the other two directions. The z stress is tensile near the left and right free edges and compressive in the middle of the wall. Because there is no net force applied to the wall in the z direction, the area under the σ_{zz} vs. y curve is zero.

The stresses plotted in Fig. 3 were measured on a thin wall that was still attached to the large base plate it was built upon. One possible source of the tensile σ_{zz} stresses in the plot of Fig. 3 is constraint from the comparatively stiff base plate keeping the wall from experiencing a bending-type deformation. In this case, the base plate would induce tensile stresses on the outside edges of the plate and compressive stresses in its middle, as is seen in the stresses plotted

in Fig. 3. However, in this particular case, the wall has a large height relative to its width. This would tend to limit the effect of the base plate on the stresses at the wall's mid-height. An analogous source of the tensile σ_{zz} stresses plotted in Fig. 3 could be constraint from the portion of the wall below the location where the stresses are measured. If a wall is tall compared to its width, the wall can constrain its own bending-type deformation, setting up stresses that have a distribution like that seen in Fig. 3. A final possible cause of the σ_{zz} stresses is the increase in melt pool size near the free edge. Elevated temperatures along the vertical edge could result in the build-up of tensile stress in the vertical direction as the free-edge region cools. In this scenario, smaller contractions in the z direction in the bulk of the wall would constrain larger contractions in the z direction near the free edge, inducing tensile stresses in the free edge region. As a thin wall is constructed, this sequence of events would occur with the deposition of each wall layer.

The primary motivation of this work is to understand increases in melt pool size near free edges in the LENS™ and other similar processes, and how such increases can be controlled via dynamic decreases in laser power. A secondary issue to be considered is the existence of measured tensile stresses near the free edge in thin-walled structures and whether control of melt pool size could reduce or eliminate them.

Melt isotherm (1650 K)
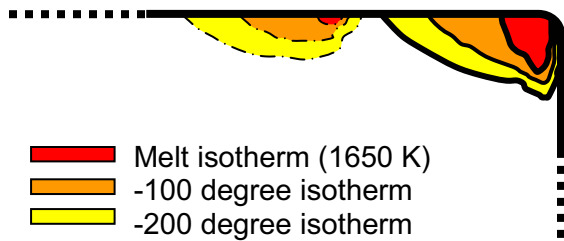-100 degree isotherm
-200 degree isotherm

Figure 2 Temperature contour plot from thermal imaging experiments on a thin wall, showing significant melt pool size increase near a free edge (from Rangaswamy et al, 2003).
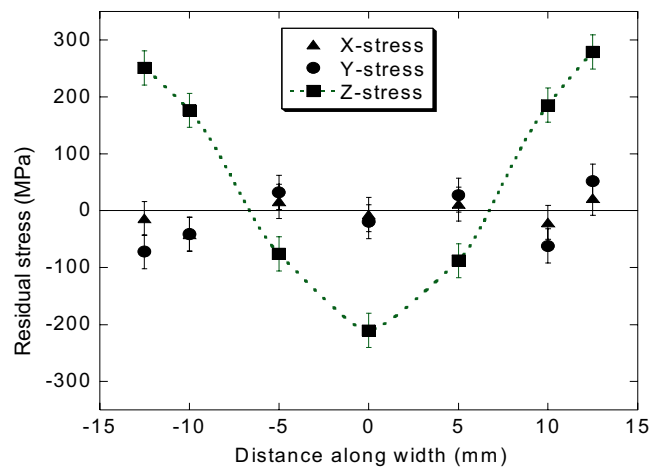
Figure 3 Plot of residual stress measured in a LENS™-deposited thin wall as a function of distance along the wall width (from Rangaswamy et al, 2003).

Existing Work: Most experimental and modeling research on automated laser-based fabrication processes has addressed the manipulation of process parameters for process control under steady build conditions. Over the past eight years, an extensive research effort to develop the LENS™ process at Sandia Laboratories has resulted in an understanding of what process parameters are needed to build a number of standard shapes out of stainless steel, titanium and a few other alloys. Despite this success, gaining a fundamental understanding of the inter-related effects of process variables such as laser power and velocity on critical process parameters such as melt pool size and residual stress remains a challenge. Such an understanding is needed to further develop LENS™ and other related laser-based freeform fabrication processes.

Modeling work by Vasinonta et al. (1999, 2001a, 2001b) has begun to address this need by developing easy-to-use "process maps" allowing the prediction of steady-state melt pool size in thin-walled and bulky features for any practical combination of LENS^{TM} process variables. The simultaneous control of residual stress and melt pool size has been addressed by Vasinonta et al. (2000). A brief overview of the process map approach to understanding laser-based freeform fabrication processes is given by Beuth and Klingbeil (2001) and a complete presentation of the process map approach for controlling steady-state melt pool size and residual stress in thin-walled and bulky parts is given by Vasinonta (2002). Most of the numerical approaches used in the research described in this paper are based on this earlier work. A new application of the process map approach involves developing process maps of cooling rates and thermal gradients at the melt pool boundary with the goal of predicting microstructure (Bontha and Klingbeil, 2003) (also in this symposium proceedings). The ultimate goal of this body of research is to understand in a fundamental way the control of melt pool size, stress and material properties in laser-based deposition processes and to present results in a form that process engineers can readily use. Portions of this research also make use of results presented in insightful internal reports from Sandia Laboratories by Dobranich and Dykhuizen (1998a, 1998b) and Dykhuizen and Dobranich, (1998). Their steady-state analytical and numerical simulations address the importance of a number of simplifying assumptions used in modeling the LENS™ process.

Although an understanding of steady-state process control is important, ultimately an understanding of dynamic process control is needed to advance laser-based freeform fabrication processes. Experimental studies of the LENS™ process by Griffith el at. (1999) and Hofmeister et al. (2001) have addressed this issue by considering transient control of melt pool size via a thermal imaging feedback control system. Their control system has the ability to alter process parameters as needed to maintain a consistent melt pool size. The research described in this paper represents an initial effort to model transient changes in melt pool size for a commonly encountered event (the approach of a free edge). Conclusions from this paper have served as the basis for developing process maps for transient melt pool size control, which is addressed in another paper in this symposium (Birnbaum et al., 2003).

Modeling Approach
The ABAQUS finite element software package was used for calculating temperatures and stresses in a thin wall. The 2-D model consists of a concentrated heat source moving across a tall thin wall 25.4 mm in length with a thickness of 1.5 mm and a height of 90 mm. These dimensions match those of the thin wall used to develop the neutron diffraction results plotted in Fig. 3. In all simulations presented in this paper, the heat source begins at the left edge of the wall, travels left to right across the wall to the right free edge, and then traverses the top of the wall again, traveling from right to left. As such, only the final pass of the laser over the wall is modeled (where the thin wall studied by Rangaswamy et al. (2003) was built up via multiple laser passes).

A moving heat source is simulated by applying a concentrated heat flux at a node on the model surface for a time equal to the distance between model nodes divided by the laser velocity. Nodal temperature results of the current step are then used as initial conditions for the next step, where a new concentrated heat flux is applied to the next node. A mechanical model of the same

mesh density and dimensions is used to simulate residual stresses caused by time-dependent temperatures from the thermal model. Meshes used for the thermal and mechanical simulations contained 32218 nodes and 31860 elements and an image of the region near the melt pool in the middle of the wall is included as part of Fig. 4. Although meshes are sufficiently dense to capture melt pool size and shape in all regions of the model, a higher density mesh is used near the right free edge, where explicit values of melt pool depth are extracted. In all simulations presented herein, deposition of 316 stainless steel is modeled (matching the experiments in Rangaswamy et al., 2003).

Figure 4 gives the boundary conditions used in the thermal and mechanical simulations. Thermal simulations model all free edges as insulated boundaries, neglecting convection and radiation at these locations, as suggested in the work by Dobranich and Dykhuizen (1998a). A fixed temperature condition is enforced at the base of the wall, modeling the base plate the wall is deposited onto as an ideal heat sink (the base plate itself is not modeled). Mechanical simulations model the free edges as traction-free, with displacements constrained to be zero at the base of the wall, modeling the mechanical constraint of the base plate.
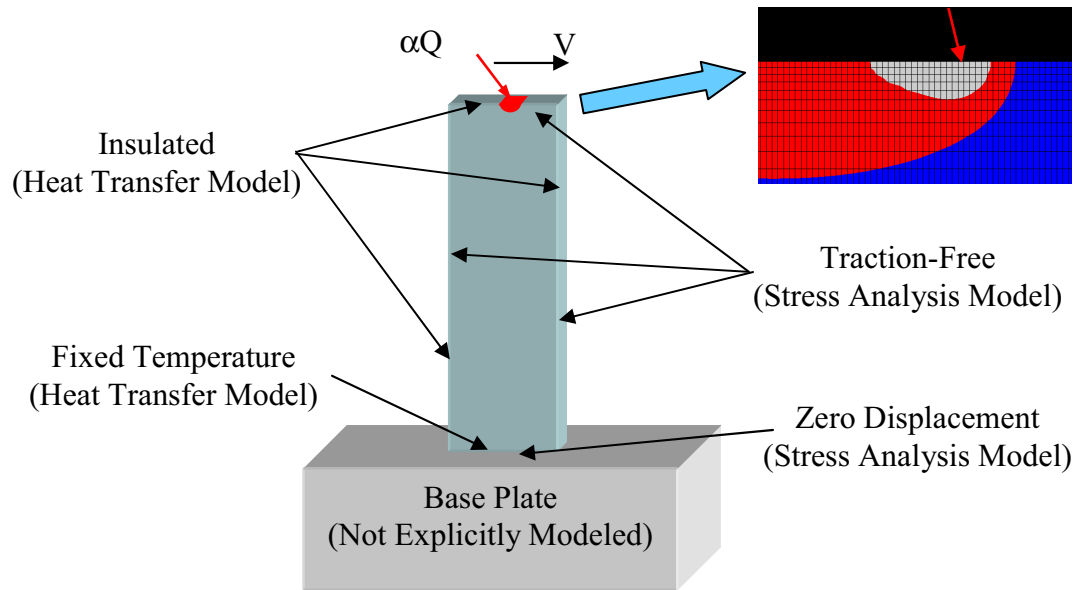

Figure 4 Schematic of the thin wall thermal and mechanical models, simulating heat transfer from a point heat source moving across the top edge and resulting thermal stresses.

Thermal properties of AISI 316 stainless steel used in the simulations include a solidus temperature of 1644 K, a liquidus temperature at 1672 K and constant density of 7652 kg/m^3 (Peckner and Bernstein, 1977). Based on data plotted by Peckner and Bernstein (1977) the variation of thermal conductivity and specific heat with temperature is approximated up to the solidus temperature by the following linear relations:

$$k = 11.82 + 0.0106\ T\ \textit{(W/mK)} \tag{1}$$

$$c = 389.66 + 0.230\ T\ \textit{(J/kgK)}\ .$$

Above the solidus temperature, k and c are held constant. A latent heat of fusion of 2.65×10^5 J/kg is also used.

Mechanical properties used in the simulations are also taken from Peckner and Bernstein (1977). The Young's modulus and coefficient of thermal expansion are approximately linear functions of temperature and are represented by the following equations:

$$E = 200 - 0.094(T\text{-}300)\ \text{GPa} \tag{2}$$

$$\alpha = 14.55 + 0.0037T \quad 10^{-6}/\text{K}$$

Above the solidus temperature, the Young's modulus and coefficient of thermal expansion are held constant at 1 GPa and 20.6×10^{-6}/K, respectively. The temperature dependence of yield stress is taken from tabulated data of yield stress divided by room temperature yield stress. A room temperature yield stress of 441 MPa was used, as measured for LENS$^{\text{TM}}$-deposited SS 316 (Griffith et al., 1996).

Process Maps for Melt Pool Size
As shown by Vasinonta et al. (1999, 2001a), the solution of Rosenthal (1946) for a point heat source moving across a (2-D) half-space can be used as the basis for developing "process maps" that rigorously quantify the relationship between melt pool size and laser power, laser speed, part height and part preheat temperature. Although the process maps are strictly applicable to steady-state thermal conditions, in this paper they are used as a guide for determining power reductions needed to maintain a constant melt pool size under transient conditions as a free edge is approached. As suggested by the Rosenthal (1946) solution, a process map for melt pool length in thin-walled structures is represented through three dimensionless variables: the normalized melt pool length, $\bar{l}$, the normalized substrate height, $\bar{h}$, and the normalized melting temperature, $\bar{T}_m$, which are defined as follows:

$$\bar{l} = \frac{l}{2k / \rho c V}, \quad \bar{h} = \frac{h}{2k / \rho c V} \quad \text{and} \quad \bar{T}_m = \frac{T_m - T_{base}}{\alpha Q / \pi k t}. \tag{3}$$

In eq. (3), l is the melt pool length, t is the wall thickness and h is the wall height. ρ, c, k and T_m are the density, specific heat, thermal conductivity and melting temperature of the deposited material, respectively. αQ is the absorbed laser power, V is the laser velocity, and T_{base} is the wall and base plate preheat temperature.

If thermal properties are temperature-independent, results from the analysis of a concentrated heat source moving over a thin-walled structure of finite height, h, can be represented as a single surface plotted on three coordinate axes of $\bar{l}$, $\bar{h}$ and $\bar{T}_m$. Vasinonta et al. (1999, 2001a) demonstrate that even for analyses including temperature-dependent properties and latent heat, results can be graphically represented in terms of these dimensionless variables with acceptable accuracy, valid of over the full range of process variables used in the deposition of stainless steel in the LENS$^{\text{TM}}$ process. Coupled with rules developed for its effective use, the resulting "process map" allows the presentation of melt pool length results for all combinations of process variables in a compact and useable form.

Modeling Results

Melt Pool Depth Control: The plots of model results in Figs. 5 and 6 demonstrate how melt pool depth can be controlled through reductions in laser power as a free edge is approached. In both figures, the term heat flux power refers to absorbed laser power, αQ, where α is taken as equal to 0.35. In this paper, melt pool depth is considered instead of melt pool length because it is potentially related to the development of tensile stresses at the free edge. Control of melt pool depth is also critical in ensuring bonding between deposited layers. As indicated by the solid red line in Fig. 5, for the case of a heat source moving toward a free edge with constant laser velocity and power (designated by the dashed red line), melt pool depth is increased by a factor of roughly 2.5. This behavior is caused by the proximity of the free edge reducing conductive heat transfer from the melt pool area.

The melt pool depth increases seen under constant power conditions (the data designated by the solid red line) have been used to estimate power reductions needed to control melt pool depth as the free edge is approached. This data has been combined with results from the process map research by Vasinonta et al., 1999, 2001a. In that work, it is shown that the Rosenthal analytical solution can be used to effectively predict melt pool length in tall walls of SS304 if properties of SS304 at 1000 K are used in calculating dimensionless variables. Based on this result, the Rosenthal solution with properties of SS304 at 1000 K (which are similar to SS316) was used to calculate the percent reduction in laser power needed to return to the ambient steady-state value of melt pool depth as a function of laser travel distance. The resulting power vs. travel distance curve is given as the black dashed line in Fig. 6. This power vs. distance curve yields a substantially smaller increase in melt pool size as the free edge is approached (the black solid line).
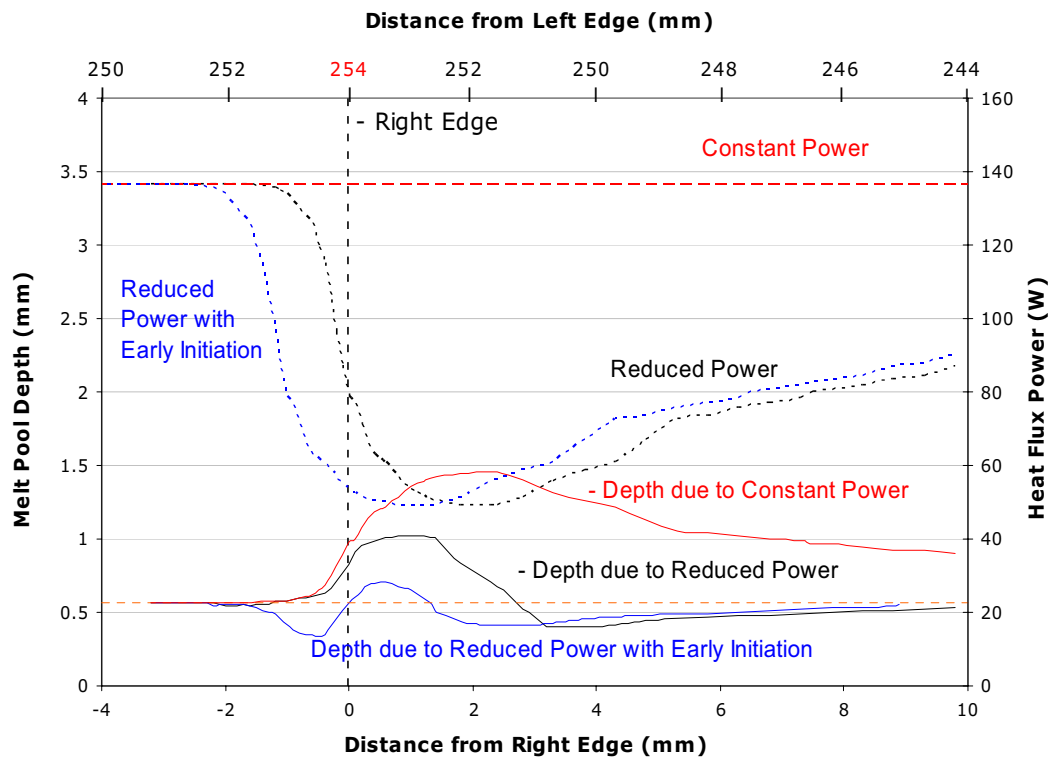

Figure 5 Melt pool depth vs. horizontal distance traveled near a free edge, for constant and varying laser powers with and without early initiation in laser power reduction.

Although it is an improvement, the melt pool size changes designated by the solid black line of Fig. 5 are still not optimal. A roughly 75% increase in melt pool depth is seen. A critical issue is the time delay between a power change at the melt pool and resulting changes in the melt pool size. The results designated by the blue dashed and solid lines illustrate an attempt to remedy this. In this case, the power reduction vs. travel distance curve, designated by the blue dashed line, is identical to the black dashed line, but the reduction in power is initiated before the melt pool size begins to increase. The resulting plot of melt pool size vs. travel distance shows an initial decrease in melt pool size, followed by a much smaller melt pool size increase. Overall, the melt pool size is near the free edge is effectively controlled.

It is important to reiterate that the power reduction curve used in this case (the blue dashed line in Fig. 5) is based on melt pool size increases under constant power conditions. Because those melt pool size increases now do not occur, the power reduction magnitudes as the laser moves away from the free edge are larger than they need to be. This is clearly seen in the melt pool size data for values of distance from the right edge greater than 2 mm. The melt pool depth does not approach its steady-state value because the power (which is based on the red solid line data) has not been increased to its steady-state value. To consider this issue, another simulation has been performed that includes not only the early initiation of power reductions, but also a sudden increase to 60% of the ambient power at the time when the melt pool depth reaches its steady-state value as it moves away from the free edge, followed by an increase to 80% of the ambient power. Figure 6 shows the results of this case, which is meant to simulate some type of feedback control of melt pool size. The resulting plot of melt pool depth shows good control of melt pool size as the laser leaves the free edge region.
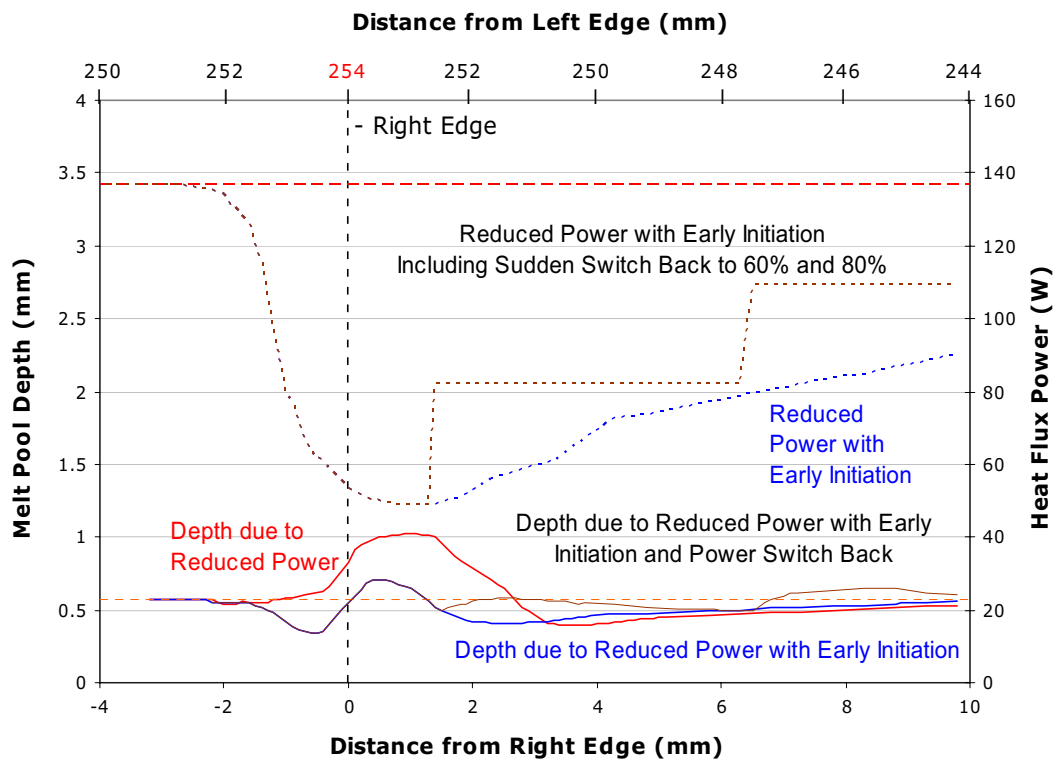

Figure 6 Melt pool depth vs. horizontal distance traveled near a free edge, for varying laser powers including one case with early initiation of power reduction and a sudden switch to 60% and then 80% of the ambient laser power.

Collectively, the results of Figs. 5 and 6 show that power reductions suggested by steady-state model results (e.g. the process maps of Vasinonta et al., 1999, 2001a) can be a useful guide for maintaining a consistent melt pool size as a free edge is approached. However, if power reductions are initiated at the time when the melt pool size begins to increase (as would be done in a feedback control system) the benefit is limited. Instead, power reductions should be initiated in advance of observed increases in melt pool size. Finally, at some point feedback control must be used to effectively return the melt pool to steady state conditions. Thus effective control of melt pool size requires a combination of accurate tracking of heat source location, accurate modeling to determine the initiation time and magnitude of power reductions, and feedback control of power based on observed melt pool sizes.

Stress Control: Figures 7 and 8 show stress contour plots in thin-walled structures after cool-down to room temperature, resulting from a heat source traveling across the top of the wall from left to right and then from right to left. The contour plot of Fig. 7, which is for the case of constant laser power, shows a significant amount of tensile residual stress in the vertical direction near the left and right edges. Although the model is for a single back and forth pass of the heat source, the resulting stresses are qualitatively similar to the experimental results plotted in Fig. 3. The contour plot of Fig. 8 is for the same case as that for Fig. 7; however, the melt pool size has been controlled near the free edges via the power reduction curve designated by the blue dashed line of Fig. 6. It is clear that the tensile stresses near the free edge are not significantly changed by controlling melt pool size (though they are reduced slightly).

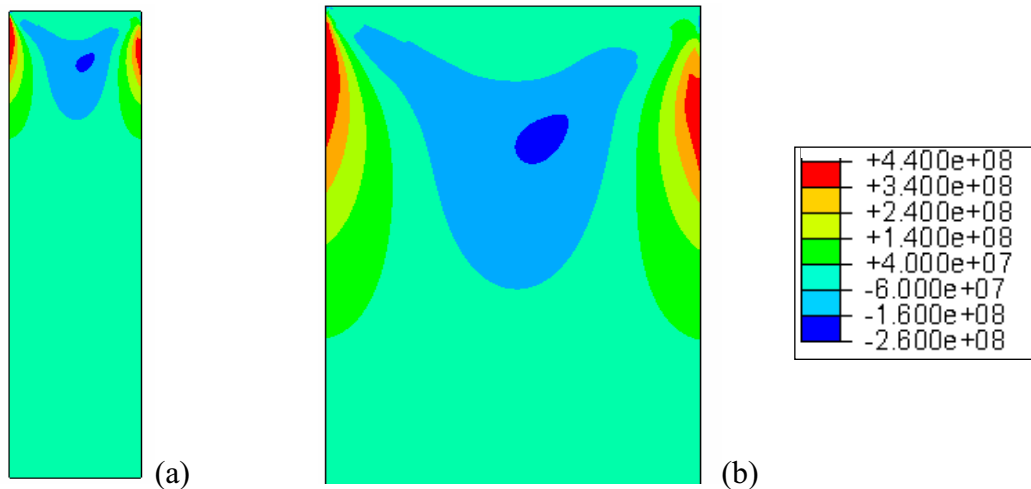(a)   (b)

Figure 7 (a) Vertical stress contours after cool-down to room temperature obtained from a model with constant laser power and (b) magnification of the top portion of the contour plot.

Finally, Fig. 9 provides a stress contour plot from an elastic thermal simulation designed to replicate the types of stresses induced in the tall wall by the laser. That simulation consists of a thermal mismatch problem, where a layer on top of the wall is subjected to a uniform free thermal contraction relative to the rest of the wall. The thickness of the layer was chosen to roughly match the thickness of the region in the top of the heat source simulation experiencing tensile stresses in the horizontal direction. The magnitude of the thermal mismatch strain was chosen to give an average stress in the layer roughly equal to the tensile stress in the horizontal direction in the top region of the heat source model. As shown in Fig. 9, the elastic simulation

clearly produces stress contours analogous to those from the heat source simulation of the thermal deposition process.
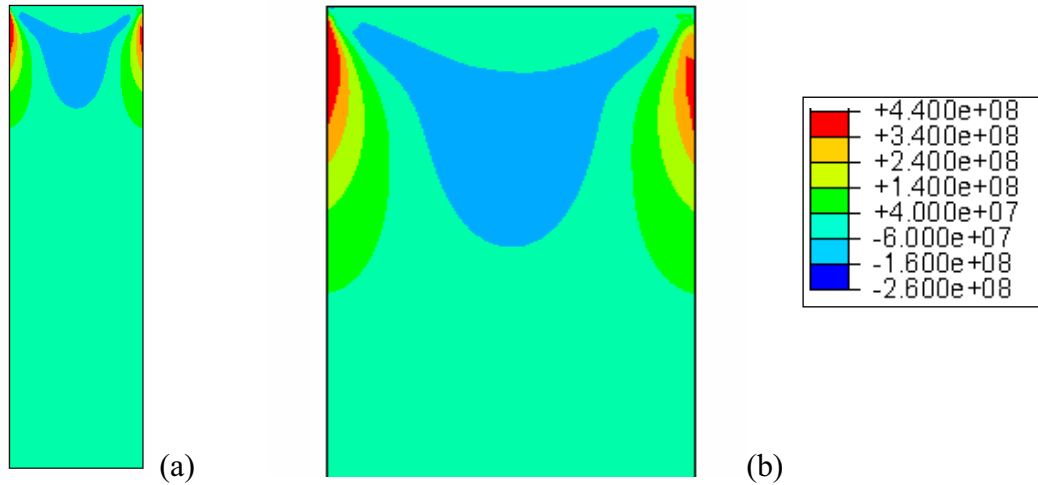

Figure 8 (a) Vertical stress contours after cool-down to room temperature obtained from a model with reduced laser power near the left and right edges (controlled melt pool depth) and (b) magnification of the top portion of the contour plot.
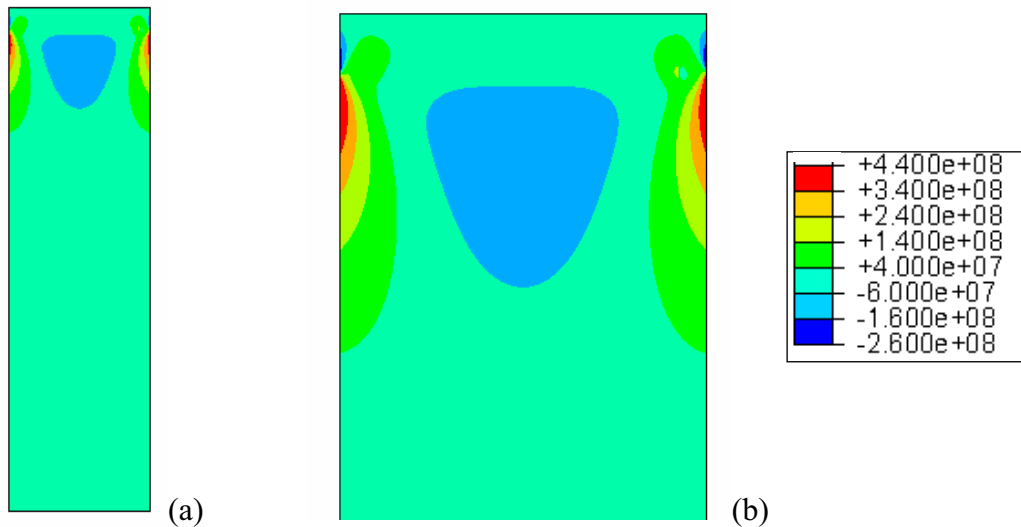

Figure 9 (a) Vertical stress contours from an elastic simulation reproducing the model cool down process and (b) magnification of the top portion of the contour plot.

The conclusion from the stress results of Figs. 7-9 is that the primary cause for measured and modeled tensile stresses in the vertical direction near the free edges of deposited thin walls is not melt pool size increases. Substantial reductions in melt pool size near the free edges yield only a minor reduction in free edge stresses. Also, the same types of stresses are seen in the elastic simulation of a thermal mismatch strain, where no melt pool exists at all. For the simulations performed in this study, constraint of the base plate is also not an issue. The walls are so tall relative to their width that the stresses at the base of the wall due to constraint of the base plate are not significant. If the constraint at the base plate were removed, the effect on the free edge stresses would be minimal. There may be some role of base plate constraint for the stresses plotted in Fig. 3, however, which were measured at a location halfway up the wall

height. The main cause for the tensile stresses in the vertical direction near the free edge appears to be constraint from bending-type deformation by the bulk of the wall below the top surface. In a tall wall built up by successive deposition of layers, one would expect tensile stresses at the free edges (and compressive stresses in the middle of the wall) along nearly the entire wall height, falling rapidly to zero as the top free edge is approached. Removal of the base plate would relax these stresses near the base of the wall only.

Conclusions

The primary goal of this research was to gain insight into how increases in melt pool size seen at free edges in the LENS^{TM} and other similar processes can be controlled. A second goal was to understand the development of tensile residual stresses measured near the free edges of thin-walled structures, determining whether control of melt pool size in that region could in turn help reduce these stresses. The modeling work performed in this research demonstrates that power vs. melt pool size relationships developed from steady-state models can be used as a guide in determining power reductions needed to maintain a consistent melt pool size as a free edge is approached. However, if one waits until an increase in melt pool size begins to occur before initiating power reductions (as is done in feedback control systems) melt pool size cannot be effectively controlled. Instead, power reductions should be initiated in advance of melt pool size changes to compensate for the time required for system response to laser power changes. Thus, a key component of melt pool size control is effective process modeling to determine appropriate power changes and distances from the free edge to initiate them. As the laser leaves the free edge, feedback control becomes important to achieve a rapid return to steady-state conditions.

Mechanical models have determined that localized increases in melt pool size are not the primary cause for large magnitude tensile stresses measured in the vertical direction near free edges. Instead, these stresses are primarily caused by constraint of the wall from a bending type of deformation. If a wall is short compared to its width, or at the base of a tall wall, the constraint will come from the large base plate the wall is deposited onto. Away from the base of tall walls, tensile stresses near the free edges are induced by constraint of the wall itself. These stresses will remain even after the wall is machined from the base plate.

References
 1. Beuth, J.L. and Klingbeil, N.W., 2001, "The Role of Process Variables in Laser-Based Direct Metal Solid Freeform Fabrication," *JOM,* September 2001, pp. 36-39.
 2. Birnbaum, A., Aggarangsi, P. and Beuth, J.L., 2003, "Process Scaling and Transient Melt Pool Size Control in Laser-Based Additive Manufacturing Processes, " *Solid Freeform Fabrication Proceedings* (D.L. Bourell, J.J. Beaman, H.L. Marcus, R.H. Crawford and J.W. Barlow, eds.), Proc. 2003 Solid Freeform Fabrication Symposium, Austin, August 2003 (this symposium).

3. Bontha, S. and Klingbeil, N.W., 2003, "Thermal Process Maps for Controlling Microstructure in Laser-Based Solid Freeform Fabrication," *Solid Freeform Fabrication Proceedings* (D.L. Bourell, J.J. Beaman, H.L. Marcus, R.H. Crawford and J.W. Barlow, eds.), Proc. 2003 Solid Freeform Fabrication Symposium, Austin, August 2003 (this symposium).

4. Dobranich, D. and Dykhuizen, R. C., 1998a, "Scoping Thermal Calculation of the LENS™ Process," Sandia National Laboratories Internal Report, 1998.

5. Dobranich, D. and Dykhuizen, R. C., 1998b, "Analytical Thermal Models for the LENS™ Process," Sandia National Laboratories Internal Report.

6. Dykhuizen, R. C., and Dobranich, D. 1998, "Cooling Rates in the LENS™ Process," Sandia National Laboratories Internal Report.

7. Griffith, M.L., Keicher, D.M., Atwood, C.L., Romero, J.A., Smugeresky, J.E., Harwell, L.D. and Greene, D.L., 1996, "Freeform Fabrication of Metallic Components Using Laser Engineered Net Shaping (LENS)," *Solid Freeform Fabrication Proceedings* (D.L. Bourell, J.J. Beaman, H.L. Marcus, R.H. Crawford and J.W. Barlow, eds.), Proc. 1996 Solid Freeform Fabrication Symposium, Austin, August 1996, pp. 125-132.

8. Griffith, M. L., Schlienger, M. E., Harwell, L. D., Oliver, M. S., Baldwin, M. D., Ensz, M. T., Smugeresky, J. E., Essien, M., Brooks, J., Robino, C. V., Hofmeister, W. H., Wert, M. J. and Nelson, D. V., 1999, "Understanding Thermal Behavior in the LENS™ Process," *Journal of Materials Design,* Vol. 20, No. 2/3 pp. 107-114.

9. Hofmeister, W.H., Griffith, M.L., Ensz, M.T. and Smugeresky, J.E., 2001, "Solidification in Direct Metal Deposition by LENS Processing," *JOM*, Vol. 53, No. 9, 2001, pp. 30-34.

10. Peckner, D. and Bernstein, I. M.,1977, *Handbook of Stainless Steels,* McGraw-Hill, 1977.

11. Rangaswamy, P., Holden, T.M., Rogge, R.B. and Griffith, M.L., 2003, "Residual Stresses in Components Formed by the Laser-Engineered Net Shaping (LENS^{TM}) Process," submitted to *J. Strain Analysis*.

12. Rosenthal, D., 1946,"The Theory of Moving Sources of Heat and Its Application to Metal Treatments," *Transactions of ASME,* Vol. 68, 1946, pp. 849-866.

13. Vasinonta, A., Beuth, J. L. and Griffith, M. L., 1999, "Process Maps for Laser Deposition of Thin-Walled Structures," *Solid Freeform Fabrication Proceedings,* (D.L. Bourell, J.J. Beaman, R. H. Crawford, H. L. Marcus and J. W. Barlow, eds.), Proc. 1999 Solid Freeform Fabrication Symposium, Austin, August 1999, pp. 383-391.

14. Vasinonta, A., Beuth, J.L. and Griffith, M.L., 2000, "Process Maps for Controlling Residual Stress and Melt Pool Size in Laser-Based SFF Processes," *Solid Freeform Fabrication Proceedings* (D.L. Bourell, J.J. Beaman, R.H. Crawford, H.L. Marcus and J.W. Barlow, eds.), Proc. 2000 Solid Freeform Fabrication Symposium, Austin, August 2000, pp. 200-208.

15. Vasinonta, A., Beuth, J. L. and Griffith, M. L., 2001a, "A Process Map for Consistent Build Conditions in the Solid Freeform Fabrication of Thin-Walled Structures," *Journal of Manufacturing Science and Engineering.* Vol. 123, pp. 615-622.

16. Vasinonta, A., Beuth, J.L., and Ong, R., 2001b, "Melt Pool Size Control in Thin-Walled and Bulky Parts via Process Maps," *Solid Freeform Fabrication Proceedings* (D.L. Bourell, J.J. Beaman, R.H. Crawford, H.L. Marcus, K.L. Wood and J.W. Barlow, eds.), Proc. 2001 Solid Freeform Fabrication Symposium, Austin, August 2001, pp. 432-440.

17. Vasinonta, A., 2002, "Process Maps for Melt Pool Size and Residual Stress in Laser-Based Solid Freeform Fabrication," Ph.D. Thesis, Carnegie Mellon University, May 2002.